Synthesis and Properties of CdSe/ZnS Core/Shell Nanorods

Taleb Mokari and Uri Banin*

Institute of Chemistry, The Farkas Center for Light Induced Processes and the Center for Nanoscience and Nanotechnology, The Hebrew University of Jerusalem, Jerusalem 91904, Israel

Received March 19, 2003. Revised Manuscript Received May 29, 2003

A method for the synthesis of CdSe/ZnS core/shell nanorods is reported. In the first step rods are grown, and in a second step a shell of ZnS is overgrown at moderate temperatures in a mixture of trioctylphosphine-oxide and hexadecylamine. Structural and chemical characterization using transmission electron microscopy, X-ray diffraction, and energy dispersive X-ray spectroscopy were performed providing direct evidence for shell growth. The emission quantum yield significantly increases by over 1 order of magnitude for the core/shell nanorods compared to the original rods because of the improved surface passivation. Rods with lengths up to ∼30 nm were investigated, and in this size regime the maximal achievable QY showed little dependence on length and strong dependence on rod diameter, with increased QY in smaller diameters. Color tunability is available via tuning of the rod diameter. The stability against photooxidation was significantly improved in core/shell nanorods compared with rods coated by organic ligands.

Introduction

Shape control of colloidal semiconductor nanocrystals has been recently achieved by modifying the synthesis to obtain rod shaped particles—quantum rods (QRs).[1−5] Such QRs display the transition from zero-dimensional quantum dots (QDs), to one-dimensional quantum wires in the sense that the length becomes a weakly confined axis.[6−8] QRs show several advantages over spherical nanocrystals for serving as novel materials for laser applications. In a recent study, lasing was detected for CdSe rods overcoated by a thin ZnS shell, and the lasing threshold was found to be significantly reduced compared to the threshold for spherical QDs.[9] Color control is available through the control of the rod diameter that was found to govern the band gap energy of CdSe QRs. Additionally, polarized emission was detected for rods related with their cylindrical symmetry.[10,11] These favorable characteristics of QRs as laser materials provide clear motivation for improvements in their emission quantum yield and photostability while still maintaining the basic rod architecture. In this paper we describe the preparation and characterization of CdSe/ZnS core/shell nanorods of various lengths and diameters with high emission quantum yields (QY) and greatly improved photostability as compared with organically coated core rods.

For spherical semiconductor nanocrystals, a proven strategy for increasing both the fluorescence QY and the stability is to grow a shell of a higher band gap semiconductor on the core nanocrystal.[12−21] If the band-offsets between the core and shell materials are such that the band-gap of the core is enclosed by that of the shell, a configuration known as type I, then the electron and hole wave functions may be confined to the core region, reducing the probability for nonradiative decay via surface states and traps. Such core/shell nanocrys-

* To whom correspondence should be addressed: banin@chem.ch.huji.ac.il.

(1) Peng, X. G.; Manna, L.; Yang, W. D.; Wickham, J.; Scher, E.; Kadavanich, A.; Alivisatos, A. P. *Nature* **2000**, *404*, 59.
(2) Kan, S. H.; Mokari, T.; Rothenberg E.; Banin U. *Nature Mater.* **2003**, *2*, 155.
(3) Tang, Z. Y.; Kotov, N. A.; Giersig, M. *Science* **2002**, *297*, 237.
(4) Pacholski, C.; Kornowski, A.; Weller, H. *Angew. Chem., Int. Ed.* **2002**, *41*, 1188.
(5) Kim, Y. H.; Jun, Y. W.; Jun, B. H.; Lee S. M.; Cheon, J. W. *J. Am. Chem. Soc.* **2002**, *124*, 13657.
(6) Li, L. S.; Hu, J. T.; Yang, W. D.; Alivisatos, A. P. *Nano Lett.* **2001**, *1*, 349−351.
(7) Katz, D.; Wizansky, T.; Millo, O.; Rothenberg, E.; Mokari, T.; Banin, U. *Phys. Rev. Lett.* **2002**, *89*, 086801.
(8) Hu, J. T.; Wang, L. W.; Li, L. S.; Yang, W. D.; Alivisatos, A. P. *J. Chem. Phys.* **2002**, *106*, 2447.
(9) Kazes, M.; Lewis, D. Y.; Ebenstein, Y.; Mokari, T.; Banin, U. *Adv. Mater.* **2002**, *14*, 317.
(10) Hu, J.; Li, L. S.; Yang, W.; Manna, L.; Wang, L. W.; Alivisatos A. P. *Science* **2001**, *292*, 2060.
(11) Chen, X.; Nazzal, A.; Goorskey, D.; Xiao, M.; Peng, Z. A.; Peng, X. *Phys. Rev. B* **2002**, *64*, 245304.
(12) Mews, A.; Eychmüller, A.; Giersig, M.; Schoos, D.; Weller, H. *J. Phys. Chem.* **1994**, *98*, 934.
(13) Hines, M. A.; Guyot-Sionnest, P. J. *J. Phys. Chem.* **1996**, *100*, 468.
(14) Peng, X.; Schlamp, M. C.; Kadavanich, A. V.; Alivisatos, A. P. *J. Am. Chem. Soc.* **1997**, *119*, 7019.
(15) Dabbousi, B. O.; Rodriguez-Viejo, J.; Mikulec, F. V.; Heine, J. R.; Mattoussi, H.; Ober, R.; Jensen, K. F.; Bawendi, M. G. *J. Phys. Chem. B.* **1997**, *101*, 9463.
(16) Tian, Y.; Newton, T.; Kotov, N. A.; Guldi, D. M.; Fendler, J. H. *J. Phys. Chem.* **1996**, *100*, 8927.
(17) Cao, Y. W.; Banin, U. *Angew. Chem. Int. Ed.* **1999**, *38*, 3692.
(18) Kershaw, S. V.; Burt, M.; Harrison, M.; Rogach, A.; Weller, H.; Eychmuller, A. *Appl. Phys. Lett.* **1999**, *75*, 1694.
(19) Cao Y. W.; Banin, U. *J. Am. Chem. Soc.* **2000**, *122*, 9692.
(20) Talapin, D. V.; Rogach, A. L.; Kornowski, A.; Haase, M.; Weller, H. *Nano Lett.* **2001**, *1*, 207.
(21) Harrison, M. T.; Kershaw, S. V.; Rogach, A. L.; Kornowski, A.; Eychmuller, A.; Weller, H. *Adv. Mater.* **2000**, *12*, 123.

10.1021/cm034173+ CCC: $25.00
Published on Web 09/13/2003

tals have proven useful in applications of nanocrystals as biological fluorescence markers,[22,23] and as chromophores in visible and NIR light emitting diodes (LEDs).[24]

This calls for an effort of developing a synthesis of core/shell nanorods with characteristics similar to those found in their spherical analogues' while still maintaining the basic rod architecture. This presents a significant synthetic challenge, as there is a requirement to maintain the rod shape even though it is not the thermodynamically stable configuration. To this end, Scher et al. recently reported the synthesis of graded CdSe/CdS/ZnS core/shell nanorods that, after photochemical annealing, display high fluorescence QY in the range of 15−20%.[25] Here we report on a different approach for growth of CdSe/ZnS core/shell nanorods that does not involve photochemical annealing. The core/shell nanorods synthesized by this method exhibit QY in the range of 20−30% and the dependence of the QY on rod length and diameter was investigated. We found that the core/shell nanorods are significantly more stable against photo degradation than CdSe rods overcoated by organic ligands.

Materials and Methods

Chemicals for Synthesis of Core/Shell Nanorods. Dimethylcadmium ($Cd(CH_3)_2$) and tri-*n*-butylphosphine (TBP, 99%) were purchased from Strem. $Cd(CH_3)_2$ was vacuum transferred from its original cylinder to remove impurities, and stored in a refrigerator inside the glovebox. Tetradecylphosphonic acid (TDPA) was purchased from Alfa. Hexylphosphonic dichloride ($C_6H_{13}Cl_2PO$, 95%), trioctylphosphine (TOP, 90% purity), trioctylphosphine oxide (TOPO, 90% purity), selenium (Se), hexamethyldisilathiane {$(TMS)_2S$}, 1 M diethylzinc {$Zn(Et)_2$} in hexane solution, anhydrous methanol, and anhydrous toluene were purchased from Aldrich. TOP was purified by vacuum distillation and kept in the glovebox. Hexylphosphonic acid (HPA) was prepared by reacting hexylphosphonic dichloride with water. Solid HPA was extracted with diethyl ether and isolated by evaporation of the solvent.

Stock Solution of CdSe Rods. Two methods were used. Method A: 0.164 g of $Cd(CH_3)_2$ (1.15 mmol) and 0.09 g of Se (1.15 mmol) were dissolved in 2.8 g of TBP (16.4 mmol) or TOP, yielding a Cd/Se ratio of 1:1. Method B: Two types of stock solutions were used. For the stock solutions for rod nucleation, $Cd(CH_3)_2$ and Se were dissolved in TBP in separate flasks, where the Cd solution was 0.162 g (1.13 mmol) of $Cd(CH_3)_2$ in 0.34 g of TBP (2 mmol), and the Se solution was 0.064 g of Se (0.81 mmol) dissolved in 1.45 g of TBP (8.5 mmol). For rod growth, 0.03 g of $Cd(Me)_2$ (0.21 mmol) was dissolved in 0.12 g of TBP (0.7 mmol) and Se solution was 0.0168 g of Se (0.21 mmol) in 0.13 g of TBP (0.76 mmol). All solutions were kept in a refrigerator at −30 °C.

Growth Solution for Rods. The growth solution for rods contained TOPO and phosphonic acid. The amounts used were 4 g of TOPO (10.3 mmol) with 8% HPA (by weight, 20% by mol), or 13% TDPA (by weight, 20% by mol).

Stock Solution for Shell Growth. ZnS shell stock solution was prepared by mixing 4 mL of TOP, $(TMS)_2S$ solution ,and 1 M $Zn(Et)_2$ hexane solution with molar ratio 2:1. The amount of $(TMS)_2S$ depends on the required shell thickness and on the initial mole amount of the core.

Synthesis of CdSe Nanorods. Two methods were used to prepare CdSe rods, as reported in earlier work.[26,27] Briefly, 4 g of TOPO and 0.32 g (20% by mole) of HPA or 0.52 g (20% by mole) of TDPA were heated in a three-necked flask on a Schlenk line under Ar atmosphere to a temperature of 360 °C with vigorous stirring.

In method A, utilizing a single stock solution that was mentioned in method A in the Stock Solution of CdSe Rod section,[26] 2 g of cold stock solution was rapidly injected and the solution was cooled to 290 °C. Further growth began two minutes after the first injection, by dropwise addition of required amount (depending on the required size) of CdSe stock solution (using a Cd/Se molar ratio of 1:1) at an approximate rate of 0.25 mL/min followed by 30 min. of annealing.

In method B for synthesizing CdSe rods, utilizing two-stock solutions,[27] the Cd stock solution was added dropwise at 360 °C and one minute later the Se stock solution was injected rapidly and the solution was cooled to 290 °C. After 20 min rods can be grown further by adding Cd growth solution, followed by addition of the Se growth solution 2 min later (the molar ratio Cd/Se is 1:1), repeating such injections for achieving the required length after a waiting time of 40 min. The reaction was stopped 30 min after the last injection. Growth was monitored by taking the absorption spectra of aliquots extracted from the reaction solution. Upon reaching the desired rod size, the reaction mixture was allowed to cool to room temperature.

The size distribution of the rods was measured from TEM images by measuring at least 200 particles and fitting the length and diameter histograms to a Gaussian distribution. In a typical reaction the size distribution was on the order of ±10% for the diameters and ±15% for the lengths.

Shell Growth. CdSe nanorods (0.1−0.4 μmol) were used for growing ZnS shells. In a typical preparation 2 g of rod sample without separation and 1 g of hexadecylamine (HDA) were heated in a three-necked flask to 120 °C for 20 min under Ar flow on a Schlenk line. The rods concentrations were calculated from the optical densities of the solutions. The molar extinction coefficient for each size was determined by a set of measurements of optical density, for quantitatively diluted solutions of rods of measured weight. For this, the rods were re-precipitated by methanol to remove excess TOPO from their powders. Three to four repetitions of this kind of measurement were carried out for each size to reduce the error. The molar weight for each rod sample was calculated using the radius and length of the rods (as determined by TEM), assuming a cylindrical shape. We summed the mass of the CdSe units and of the TOPO ligands on the rod surface assuming that half of the surface atoms are bound to TOPO.[28,29] We estimated the uncertainty in this procedure for determining rod concentration to be about ±25%.

In the next step, the nanocrystal solution was heated to 190 °C and the shell precursor solution was introduced into the hot solution by dropwise addition. The growth of core/shell nanorods was monitored by UV−Vis and photoluminescence (PL) spectroscopy of aliquots taken from the reaction flask. After growing the desired shell thickness, as calculated from the amount of rods and the lattice spacing of the (111) ZnS planes, assuming 100% yield for shell growth, the reaction mixture was cooled to room temperature. On the basis of this calculation, shell thickness is reported in monolayers (ML), where 1 ML is equal to the d_{111} lattice spacing of the shell material (d_{111} = 3.1 Å for ZnS).

Characterization. UV−Vis absorption spectra were measured using a Shimadzu UV1601. Nanocrystals were dissolved in toluene for the measurement. Photoluminescence (PL)

(22) Bruchez, M.; Moronne, M.; Gin, P.; Weiss, S.; Alivisatos, A. P. *Science* **1998**, *281*, 2013.
(23) Chan, W. C. W.; Nie, S. *Science* **1998**, *281*, 2016.
(24) Tessler, N.; Medvedev, V.; Kazes, M.; Kan, S. H.; Banin, U. *Science* **2002**, *295*, 1506.
(25) Manna, L.; Scher, E. C.; Li, L.-S.; Alivisatos, A. P. *J. Am. Chem. Soc.* **2002**, *124*, 7136.
(26) Manna, L.; Scher, E. C.; Alivisatos, A. P. *J. Am. Chem. Soc.* **2000**, *122*, 12700.
(27) Peng, Z. A.; Peng, X. *J. Am. Chem. Soc.* **2001**, *123*, 1389.
(28) Katari, J. E. B.; Colvin, V. L.; Alivisatos, A. P. *J. Phys. Chem.* **1994**, *98*, 4109.
(29) Becerra, L. R.; Murray, C. B.; Griffin, R. G.; Bawendi, M. G. *J. Chem. Phys.* **1994**, *100*, 3297.

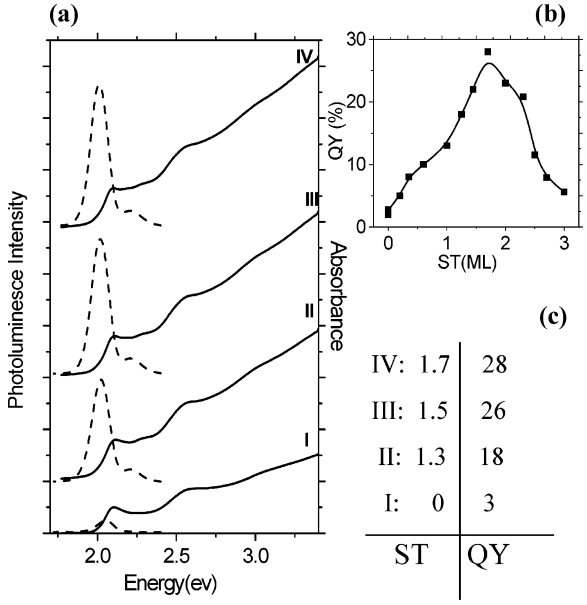

Figure 1. (a) Evolution of absorption (solid lines), and photoluminescence (dashed lines) during shell growth. (b) QY as a function of the shell thickness. (c) Increase of the QY during the shell growth, along with nominal shell thickness (ST) in monolayers corresponding to the traces shown in (a). The core rod size was 22 × 4 nm.

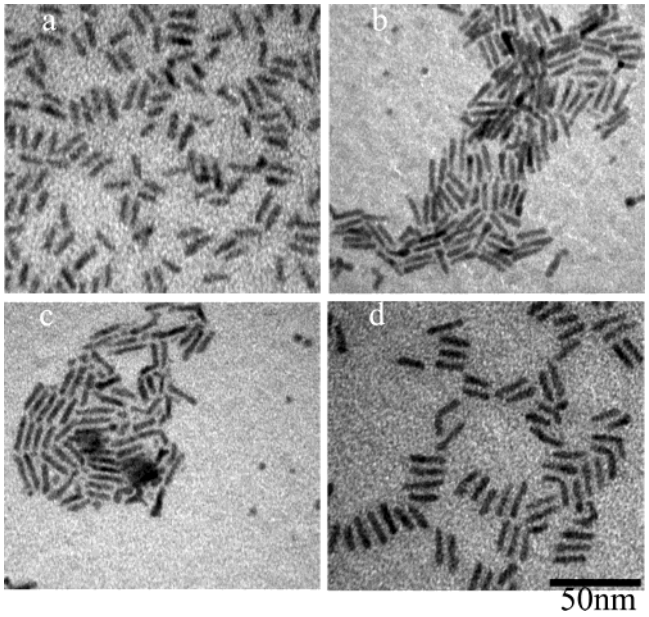

Figure 2. TEM images of rod and core/shell nanorod samples. (a) Rods 22 × 4 nm. (b−c) Core/shell nanorod samples that were grown from rods shown in (a), with shell thicknesses of 1.7 and 3.5 monolayers (ML), respectively. Dots can be seen in both samples. (d) The sample shown in (c) after separation. The dots were removed.

experiments were performed using 473 or 532 nm for excitation. The emission was collected at a right angle configuration and detected by a spectrometer/CCD setup. Room-temperature fluorescence quantum yields (QYs) of the nanocrystal toluene solutions were determined by comparing the integrated emission with that of rodamine 6G dye methanol solutions with equal optical density at the excitation wavelength. The QY values were corrected for the differences in refractive index between toluene and methanol.[30]

Powder X-ray diffraction (XRD) patterns were measured on a Philips PW 1830/40 X-ray diffractometer with Cu Kα radiation. Approximately 10 mg of nanocrystals were dispersed in a minimum volume of toluene. The nanocrystal solution was deposited onto low scattering quartz plates, and the solvent was evaporated under mild vacuum. Low-resolution transmission electron microscopy (TEM) images were obtained using a Phillips Tecnai 12 microscope operated at 100 kV. High-resolution TEM (HRTEM) images were obtained using a Tecnai F20 electron microscope operated at 200 kV. Samples for TEM were prepared by depositing a drop of a nanocrystal solution in toluene onto a copper grid supporting a thin film of amorphous carbon. The excess liquid was wicked away with filter paper, and the grid was dried in air. Energy-dispersive X-ray spectroscopy (EDS) analyses were conducted on a JEOL-JAX 8600 Superprobe. Samples were washed thoroughly with methanol, and the powder was deposited on a graphite substrate.

Results and Discussion

Synthesis Method. In the first step of the preparation of core/shell nanorods the desired rods were grown according to the published methods.[1,26,27] Initially, we tried to separate the rods from the growth solution by adding toluene and precipitating them by methanol, followed by centrifugation to extract the rods. After drying, the rods were redissolved again in TOPO and we grew a shell on the separated rods at 190 °C. In this approach, dissolution of the rods occurred and their morphology was not preserved, as seen from a blue shift and significant broadening of the absorption spectra. To alleviate this problem, CdSe rods were prepared and then cooled to room temperature, and without separation we continued to the next step constituting ZnS shell growth. In this case, excess unreacted precursors from the first step are present in the solution thereby suppressing rod dissolution, and the rod architecture can be maintained throughout the core/shell nanorod growth.

For core/shell nanorod synthesis, following the approach used by Weller and co-workers for spherical core/shell nanocrystals,[20] hexadecylamine (HDA, 45 wt %) was used in the growth solution. The amine is critical in order to get high QY. Prior to shell growth the rod solution was annealed at 120 °C for 20 min to allow for surface exchange from TOPO to the amine to take place. Then the temperature was raised to 190 °C for shell growth. The ZnS stock solution was added dropwise to prevent nucleation of ZnS dots. In some cases we still observed nucleation of ZnS dots but these could be easily separated after cooling by use of size-selective precipitation, as detailed below. The optimal ratio found for Zn:S was 1:2. Ratios of 1:1 or 2:1 (excess of Zn) were also attempted but resulted in lower QY.

Optical and Structural Characterization of Core/Shell Nanorods. Shell growth was monitored by measuring absorption and PL of aliquots extracted during the synthesis. Typical results for growth of a shell on rods, 22 × 4 nm (length × diameter), are presented in Figure 1a. Trace I corresponds to the core rods before adding HDA where the initial QY is 3%. After adding HDA the QY increased to ∼12%. Upon adding ZnS shell precursor stock solution, there is a considerable increase in the QY, as can be seen for traces II−IV. Trace IV represents the point of maximal QY achieved for a shell thickness of slightly less than 2

(30) Lakowicz, J. R. *Principles of Fluorescence Spectroscopy*; Kluwer Academic Publishers: New York, 1999; p 52.

Table 1. Summary of Data for Core/Shell Nanorod Samples

sample	rods size (length × diameter) (nm)	shell thickness (ML)	PL wave-length in maximum QY (nm)	maximum QY (%)	QY after separation (%)
A	11 × 3	2.3	580	40	34
B	15 × 3.8	2	614	28	19
C	22 × 4	1.7	614	28	18
D	29 × 3.7	1.9	613	27	16
E	20 × 5.5	1	630	18	11

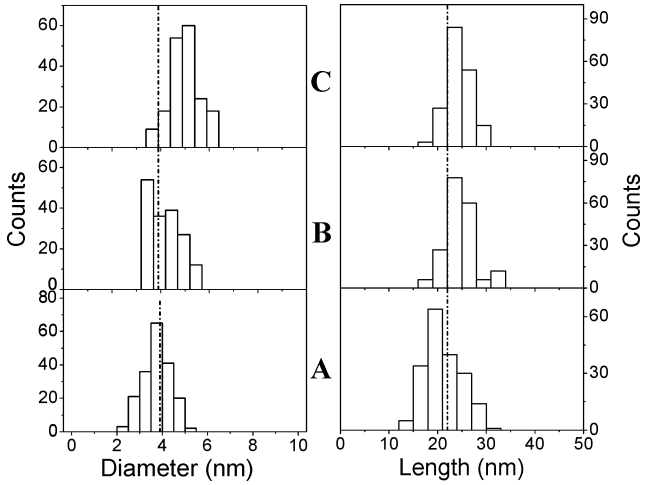

Figure 3. Size distribution of length (right frames) and diameter (left frames) of (A) rods 22 × 4 nm, (B) core/shell nanorods (ST 1.7 ML), and (C) core/shell nanorods (ST 3.5 ML) shown in Figure 2a−c, respectively.

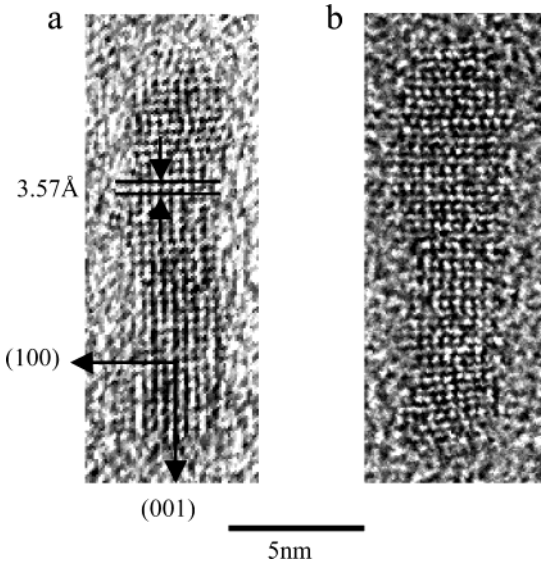

Figure 4. HRTEM images of (a) rod (14.8 × 3.4 nm), and (b) core/shell nanorod (15 × 3.7 nm).

ML, and reaching a level of 28%, reflecting an order of magnitude increase compared with the original rods without the use of photochemical annealing. Further shell growth leads to gradual reduction in the QY as can be see in Figure 1b showing the dependence of QY on nominal shell thickness. A similar trend was observed in all the samples that were measured. Such behavior was observed also previously for spherical core/shell nanocrystals and is most likely attributed to the large lattice mismatch, ~11%, between core (CdSe) and shell (ZnS) materials. While in a thin shell the strain is accommodated, further shell growth leads to defect formation that can lead to creation of traps. Upon shell growth the peak position of the PL shifts slightly to the red from 604 to 617 nm in the 2 ML shell thickness providing maximal yield (Figure 1a, trace IV). The feature on the high energy side of the emission in Figure 1a appears only for unseparated solutions and in the final product after separation is fully suppressed. It's possible assignment is to spherical dots.

The core/shell nanorod samples were characterized using TEM. Figure 2 presents the original rods (frame a), and frames b and c show core/shell nanorods with shell thicknesses of 1.7 and 3.5 ML, respectively. Dots are also resolved in both images, assigned to ZnS or alloy dot nucleation taking place upon addition of the shell precursors. These dots can be removed by size-selective precipitation. Following cooling, the core/shell nanorods are dissolved in toluene to which a small amount of methanol is added to precipitate the rods out of the growth solution. Rods, with much larger volume compared to the dots, precipitate first due to the increased Van der Walls interaction. The precipitate is separated by centrifugation and contains the rods, while the dots remain in solution. Figure 2d shows the core/shell nanorod sample after such separation was carried out.

The TEM images clearly show that our method preserves the rod architecture during shell growth. Furthermore, statistical analysis of the size distribution provides information on the increase of dimensions in both rod diameter and length upon shell growth. This analysis is summarized in Figure 3 showing the diameter and the length histograms for the original rods (Figure 3a, average size 22 × 4 nm), for the core/shell nanorod sample with shell thickness of 1.7 ML (Figure 3b, average size 24.3 × 4.2 nm), and for core/shell nanorods with shell thickness of 3.5 ML (Figure 3c, average size 24.5 × 4.9 nm). Although in this particular sample it appears that there is at first a somewhat more pronounced elongation of the rods, followed by thickening, analysis of other sizes did not reveal such an effect. For example, for sample B in Table 1, the core dimensions were 15 × 3.8 nm, and core/shell rods had dimensions of 15.5 × 4.5 nm, whereas sample D in Table 1 had a core of dimensions 29 × 3.7 nm, and core/shell rods of dimensions 31.2 × 4.7 nm.

Further characterization of the structure of core/shell nanorods was carried out by performing HRTEM measurements. Figure 4a presents an image of a rod, 14.8 × 3.4 nm, displaying cross fringes. The lattice spacing along the long axis is 3.6 Å, in agreement with the 001 lattice spacing of wurtzite CdSe. Image 4b shows a core/shell nanorod with size 15 × 3.7 nm and also here, cross fringes can be observed.

Figure 5 shows a powder XRD pattern for the rods (trace a), which agrees with the pattern of wurtzite

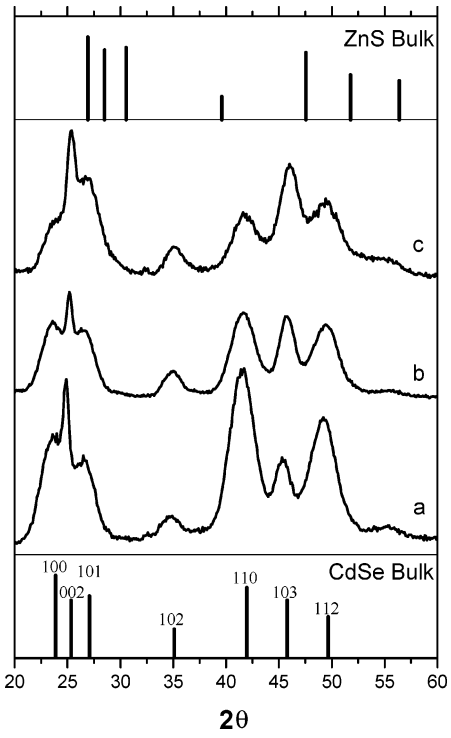

Figure 5. XRD patterns of (a) CdSe rods with size 22 × 4 nm and ZnS overcoated samples with coverage (b) 1.7 ML, (c) 3.5 ML. The lines show the peak positions for bulk wurtzite CdSe (bottom) and ZnS (top).

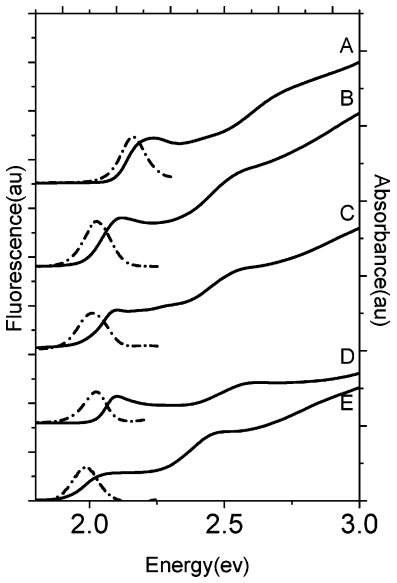

Figure 6. Absorption (solid lines) and PL (dashed lines) spectra of core/shell nanorod samples starting from rods of different sizes: (A) 11 × 3 nm, (original rod size), ST = 2.3 ML; (B) 15 × 3.8 nm, ST = 2 ML; (C) 22 × 4 nm, ST = 1.7 ML; (D) 2 9× 3.7 nm, ST = 1.9 ML; and (E) 20 × 5.5 nm, ST = 1 ML.

CdSe (bottom stick spectrum). In particular, the 002 peak is significantly narrowed compared with the other peaks, indicating that growth occurs along the 001 direction. Traces b and c show the XRD patterns for core/shell nanorods with 1.7 and 3.5 ML, respectively. Although the basic pattern is maintained upon shell growth, we observe a gradual shift of the peaks toward larger angles with the 002 peak shifting by 1.2% and 2% for 1.7 and 3.5 ML, respectively, and the 103 peak shifting by 1.1% and 1.5%, respectively. Such a shift is

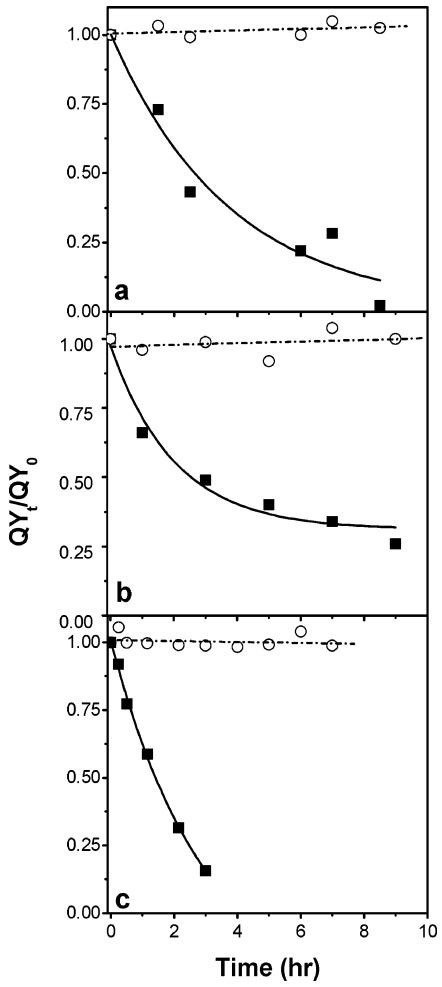

Figure 7. Photochemical stability of three rods (solid squares, solid guide lines) and core/shell nanorods (open circles, dash−dot guide lines) samples of different sizes: (a) rods (29 × 3.7 nm), core/shell nanorods (ST 1.9 ML); (b) rods (22 × 4 nm), core/shell nanorods (ST 2 ML); and (c) rods (11 × 3 nm), core/shell nanorods (ST 2.3 ML). QY_t, QY at time t, over the QY_0, at zero time, is shown versus illumination time.

expected qualitatively due to the smaller lattice constant of ZnS (bulk pattern represented by upper stick-spectrum), compared with CdSe. This kind of effect was seen previously in spherical core/shells and simulated.[19]

EDS analysis for the 22 × 4 nm rods showed an equal ratio of Cd:Se. In the core/shell nanorods with 3.5 ML shell thickness we detected a ratio of 26:21.1:25.3:27.6% for Cd/Se/Zn/S. The excess Cd and S (relative to Se and Zn, respectively) indicates a growth of a thin buffer layer of CdS before the ZnS shell grows as reported in ref 26. Although we did not add Cd during shell growth, excess Cd precursors from the stage of rod growth can react with excess S supplied for shell growth.

Size Dependence of the Quantum Yield. Similar synthesis strategy was used to grow core/shell nanorod samples on rods with different diameters and lengths. A summary of the results is presented in Table 1, and Figure 6 shows the PL (dashed lines), and the absorption (solid lines) for these samples. The peak of the PL is seen to depend primarily on diameter within the set of samples studied here, with sample A of diameter 3 nm peaking at 580 nm, samples B−D with diameter ∼3.8 nm peaking at 614 nm, and sample E with diameter 5.5 nm peaking at 630 nm. As the length in

all the studied rods is larger than the Bohr radius of bulk CdSe (5.6 nm), the length axis is weakly confined leading to a small dependence of the band gap upon length change as was observed in studies on the dependence of the optical and electronic properties of CdSe rods on dimensions.[6−8] Spectral coverage is still enabled by primarily diameter control, but it should be noted that it is difficult to prepare rods with small diameters for coverage of bluer colors.

A notable, mostly diameter-dependent trend, is observed from the data presented in Table 1. The maximal QY achieved in the core/shell nanorod samples during growth is found to mostly depend on diameter in the length regime studied here (11−∼30 nm). The highest yield is achieved for sample A (40%) with the smallest diameter; the QY is reduced for samples B−D (28%), and further reduced in sample E (18%), which has the largest diameter. Within the three samples B−D, with similar diameters, the change in length from 15 to 29 nm does not significantly affect the QY. This behavior may also reflect dominance of the strongly confined axis for determining the QY. With this size-dependent study we demonstrated that we could cover a range of wavelengths with QRs that exhibit a high QY.

Stability of Core/Shell Nanorod Samples. Aside from the increased QY, an additional stringent requirement from fluorescent nanocrystal samples is that of increased stability against photodegradation. The increased stability of spherical core/shell nanocrystals over conventional organic dyes was recently used in fluorescence marking allowing the investigation of the process of cell division.[31] We studied the issue of photostability of core/shell nanorod samples by illuminating solutions of core rods and core/shell nanorods with intense 514.5 nm light from an Ar laser at ambient conditions (room temperature, oxygen). The samples, with an optical density of 0.2, were illuminated at an intensity of 110 mw. In these conditions, the rate of absorption was estimated to be $\sim 7 \times 10^6$ photons/hour for each rod. The results are summarized in Figure 7 for three samples showing the decay in fluorescence intensity of rods versus that of core/shell nanorods. In the case of rods, a dramatic reduction in QY takes place within a time scale dependent upon rod-diameter where rods of small diameters show faster decay. All the rod samples without the shell, were seen to precipitate out of solution under these conditions and this was an irreversible process. At the same time, core/shell nanorods solutions were unaffected by the irradiation process across the entire measurement period of 10 h showing remarkable improvement in photostability. It is important to note that this kind of stability was observed only for samples that already had initial high QY (higher than ∼15%). For samples with low initial QY, we observed an increase in QY with illumination, most likely related to photochemical annealing as reported in ref 26.

(31) Dubertret, B.; Skourides, P.; Norris, D. J.; Noireaux, V.; Brivanlou, A. H.; Libchaber, A. *Science* **2002**, *298*, 1759.

Conclusions

CdSe/ZnS core/shell nanorods were synthesized and characterized. QY of up to 40% were obtained for core/shell nanorods before separation from the growth solution, and up to 34% after separation. There is a correlation between the diameter of core/shell nanorod samples and the QY, as QY is increased in small diameters. The photostability of core/shell nanorods is significantly improved compared with the stability of rods coated by organic ligands.

Acknowledgment. This work was supported in part by the Israel Ministry of Science, the Deutsche Israel program, and the James-Franck program for laser−matter interaction. We thank Yossi Larea for help with the HRTEM measurements.

CM034173+